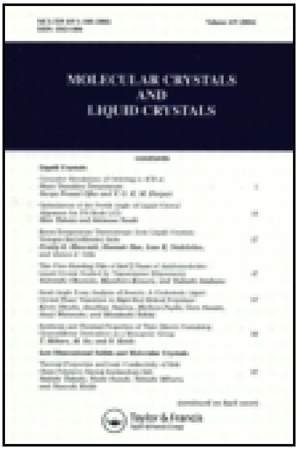

Molecular Crystals and Liquid Crystals
Publication details, including instructions for authors and subscription information:
http://www.tandfonline.com/loi/gmcl20

Effects of Thermal Conductivities of Substrates on Photothermal Self-Diffraction From Guest-Host Liquid Crystals

Hiroshi Ono [a], Takenori Takahashi [a] & Kazuaki Shibata [a]

[a] Department of Electrical Engineering, Nagaoka University of Technology, 1603-1 Kamitomioka, Nagaoka, 940-2188, Japan

Version of record first published: 18 Oct 2010

Mol. Cryst. Liq. Cryst., Vol. 392, pp. 1–15

1542-1406/03 $12.00 + .00
DOI: 10.1080/15421400390193945

EFFECTS OF THERMAL CONDUCTIVITIES OF SUBSTRATES ON PHOTOTHERMAL SELF-DIFFRACTION FROM GUEST-HOST LIQUID CRYSTALS

Hiroshi Ono, Takenori Takahashi, and Kazuaki Shibata*
Department of Electrical Engineering,
Nagaoka University of Technology,
1603-1 Kamitomioka, Nagaoka 940-2188, Japan

We report on effects of thermal conductivities of substrates on self-diffraction rings from guest-host liquid crystals (GHLCs). A He-Ne laser-induced self-phase modulation due to photothermal effects in the GHLC. A far-field pattern of the laser beam passed through the GHLC cells depended on the thermal conductivities of the substrates of the GHLC cells, and the results were well explained by three-dimensional heat-conduction analysis and Kirchhoff's diffraction theory.

Keywords: liquid crystal; self-phase modulation; photothermal effect; thermal conductivity; heat-conduction analysis

INTRODUCTION

Recent advances in the highly efficient and low-priced optical devices have renewed interest in the use of nonlinear optical effects in combination with organic materials in the field of optical information processing. Nematic liquid crystals in the mesophase have been found to exhibit extremely large laser-induced refractive index changes [1–18]. Such self-diffraction phenomena originating in self-phase modulation are readily observed through the thermally induced refractive index change in the nematic liquid crystal and have been reported by several authors [1–3,6,11–15,17,18]. Durbin et al. reported that multiple diffraction rings originating in the self-phase modulation in the nematic liquid crystal were formed by irradiation with a high-power Ar laser beam [2]. Khoo et al. reported on thermally induced

Received 17 April 2002; accepted 2 July 2002.
We thank Tokuyama Science Foundation for supporting us.
*Corresponding author. Fax: +81-47-258-9500, E-mail: onoh@nagaokaut.ac.jp

spatial transverse self-phase modulation and optical limiting of a CO_2 laser with a 100 μm liquid crystal (E7) film [4]. We demonstrated that high photosensitivity to a desired wavelength was obtained by doping with a small amount of dyes, which absorbed the laser beam [11]. The guest-host liquid crystal (GHLC) can be sensitized for writing of the laser-induced refractive index change at a desired wavelength by doping them with proper sensitizing dyes. The multiple diffraction ring pattern of a He-Ne laser beam passed through the GHLC was observed since the maximum phase increment was much larger than 2π. Macdonald et al. observed the spontaneous transverse two-dimensional optical pattern by using the GHLC in front of a single feedback mirror [13]. Among the useful nonlinear optical properties in the GHLC, the photothermal effect is the most fundamental phenomenon which allows for the realization of positive as well as negative index changes by simply changing the polarization of the input laser beam with respect to the optical axis of the birefringence liquid crystal because the gradient $\partial n_e/\partial T$ is negative while $\partial n_o/\partial T$ is positive, where n_e and n_o are the extraordinary and ordinary refractive indices, respectively. We recently published an article in which we reported that photothermal effects in the GHLC have been used for dynamic all-optical focal length converter [14]. We have presented an all-optical focal length converter using both large optical nonlinearity and anisotropic complex refractive indices in the GHLC. The polarization direction of the pump beam was controlled to be parallel to the liquid crystal director (extraordinary wave) and perpendicular to the probe beam (ordinary wave). The nonlinear phase modulation in the GHLC was generated by absorbing the pump beam, and the focal length of one laser source was varied over a range of several centimeters by changing the intensity of another laser. In order to realize such above-mentioned photonics applications using the GHLC, it is very important to investigate the mechanism of laser-induced index change in the GHLC. The photothermal effect is the most fundamental phenomenon, and it is necessary to clarify the photothermal effect because such materials absorb the laser beam. Recently, we attempted to characterize the photothermal self-phase modulation in the GHLC by analytically solving Kirchhoff's diffraction integral [12], and we also reported that photothermal self-phase modulation was well characterized by three-dimensional heat-conduction analysis [15,17,18]. We also investigated the effects of the liquid crystal cell parameters on photothermal self-phase modulation [18].

The purpose of the present study is to clarify the relationship between the photothermal effect and the thermal conductivities of the substrates. A detailed analysis of the recently proposed results [18] for the effects of cell parameters on photothermal refractive index change in the GHLC is presented here. The thermal conductivities of the cell substrates strongly affected both the time-independent and time-dependent temperature distributions in the GHLC cell, and the experimental results were well-explained by time-independent and time-dependent heat-conduction analysis.

EXPERIMENTS

Samples

The nematic liquid crystal (4′-pentyl-4-biphenylcarbonitrite, 5CB) was obtained from Merck Japan Ltd. The nematic-isotropic transition temperature of the 5CB is 36°C according to the physical characteristic data provided by the manufacturer. Commercially available Disperse Blue 14 (DB14) was obtained from Aldrich Company, Ltd. (United States) and was used as the guest dye without further purification. The chemical structures of the 5CB and DB14 are described in Figures 1(a) and 1(b), respectively. Poly(vinyl alcohol) (PVA), which was purchased fron Kuraray Co., Ltd. (Japan) was used as a GHLC alignment polymer layer. In order to clarify the relationship between the photothermal effects and the thermal conductivity of substrates, sample cells with acrylate or glass substrates were prepared. The thickness of the glass and acrylate substrates was 1.0 and 2.0 mm, respectively. The physical characteristics of 5CB, glass, and acrylate, which are provided by the manufacturer, are summarized in Table 1.

It is well known that the liquid crystal molecules are aligned on the rubbed PVA surfaces. A PVA alignment polymer layer in this study was prepared by a spin-coating method. PVA was dissolved in hot water and the solution was spun on the glass or acrylate substrates, forming an

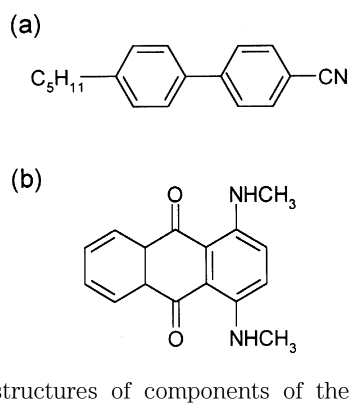

FIGURE 1 Chemical structures of components of the GHLC. (a) Host liquid crystal, 5CB and (b) guest dye, DB14.

TABLE 1 Physical Characteristics of Cell Components

	$k_{\parallel}$[J/m · K]	$k_{\perp}$[J/m · K]	ρ[g/cm^3]	c[J/g · K]
5CB	0.12	0.25	1.022	2.00
Glass	0.78	0.78	2.400	0.75
Acrylate	0.21	0.21	1.190	1.47

$k_{\parallel}$ and $k_{\perp}$ denote the thermal coductivities parallel and perpendicular to the liquid crystal director, respectively.

about 0.7 μm thick film. The resulting PVA films were dried, and two polymer-coated substrates were unidirectionally rubbed with a silk cloth in the horizontal direction. The cell was mounted with antiparallel rubbing directions and the GHLC was sandwiched with a polyester spacer. The dye concentration was 0.1 wt% and the GHLC thickness was 100 μm. A monodomain structure of two kinds of our resultant GHLC cells was observed by polarized microscope, and highly homogeneous alignment was obtained. The above procedure yields homogeneous films with good optical quality. Figure 2 shows typical absorption spectra of the two types of GHLC cells with different kinds of substrates. As shown in Figure 2, strong anisotropy exists because the 5CB and DB14 molecules are well aligned. The two samples show almost the same absorption spectra, although the different kind of the substrate is used for the GHLC cells. This material and the alignment structure are quite stable in ambient atmosphere, and its optical properties are reproducible. Although there was slight discrepancy between both results described in Figure 2, the absorption coefficients for extraordinary wave were almost equal to each other. This means that they have the same light absorption and resulting heat generation when the same power of laser beam is irradiated at both samples because the polarization is parallel to the director.

Experiment

A linearly polarized He-Ne laser (632.8 nm) was used for exciting spatial self-phase modulation in the GHLC. The laser beam was focused to an e^{-2} diameter of 137 μm at the GHLC cells. The polarization direction of the laser beam was controlled by a half-wave plate and was parallel (extraordinary) to the liquid crystal director as described in Figure 3. The laser beam was passed through the sample cell perpendicular to the glass substrate. A part of the steady-state transverse self-diffraction was cut by a pinhole and detected using a photomultiplier. The detector was interfaced to a personal computer for data acquisition and analysis. The pinhole was set on the pulse stage and one-dimensional scans of the intensity were

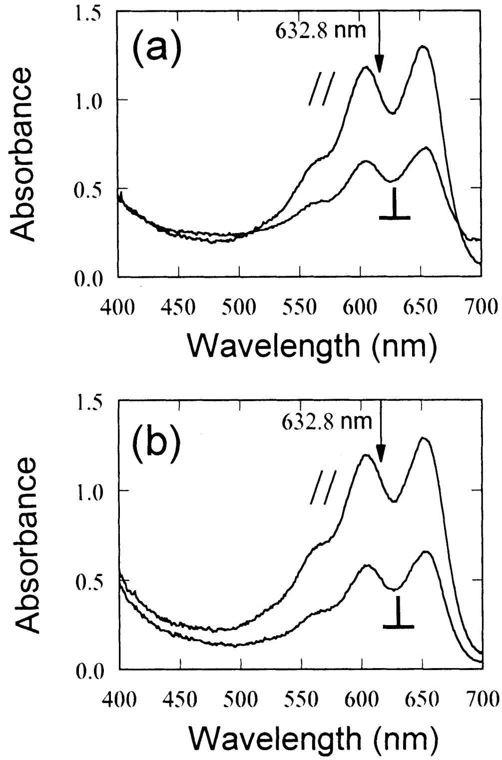

FIGURE 2 Absorption spectra of the two types of GHLC cells with different substrates. The substrate of the GHLC cell described in (a) was glass and that of the GHLC cell described in (b) was acrylate. // and ⊥ correspond to the polarizations of the probe light parallel and perpendicular to the rubbing direction (director), respectively.

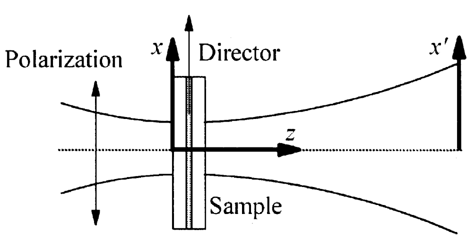

FIGURE 3 Schematic geometry of experimental characterization of photothermal effects in the GHLC cell.

obtained by varying the position of the pinhole. The transient properties of the self-phase modulation were observed as follows. The He-Ne laser beam was separated into excited and reference beams. The laser beam was switched by a mechanical shutter and the reference beam was monitored by a silicon photodiode in order to determine the time when the beam was started to incident the sample. A part of the transient diffraction beam was cut by a pinhole and guided to the photomultiplier. Both transient signals from the photodiode and the photomultiplier were monitored by Kikusui K-7101A digitizing oscilloscope. The one-dimensional scan was performed and the same transient experiment was repeated at each point. A series of the signals was reorganized into the transient fringe signal. All measurements were performed at 20°C.

RESULTS AND DISCUSSION

At a certain value of the beam intensity incident to the GHLC cell a self-diffraction process was effective, and as a result of it in a far field after the sample the diffraction ring pattern appeared. Figure 4 shows the experimental fringe signals (filled circles) and the theoretical fitted curves obtained from Kirchhoff's diffraction integral, including higher-order optical nonlinearity. It is well known that the gradient $\partial n_e/\partial T$ is negative, while $\partial n_o/\partial T$ is positive. In the case of a beam polarized parallel to the liquid crystal director, a number of diffraction rings was observed. Recently, we attempted to characterize the photothermal self-phase modulation in the GHLC by analytically solving Kirchhoff's diffraction integral and found that the higher-order optical nonlinearity could not be ignored in the GHLC [12]. The detailed method for characterizing the self-diffraction pattern was described in our previous study [12]. Note that the theoretical curve calculated on the basis of the Kirchhoff's diffraction theory is in good agreement with the experimental data. One can observe that power from the center region appears to be pushed out into the wing region as time passed. The GHLC shows large nonlinear effects and the beam characteristics were changed drastically in passage of the beam through the GHLC cells. Since DB14 does not show any photochemical and/or photophysical changes to our knowledge, we attributed the experimental results to temperature dependence of the refractive indices of the GHLC. Although the absorption coefficients and GHLC layer thickness were equal to each other, larger numbers of rings were observed in the diffraction fringes from the GHLC cell with the acrylate substrate. Since the thermal conductivity of the acrylate substrate is smaller than that of the glass substrate as described in Table 1, the heat will be accumulated in the GHLC cell with the acrylate substrate. In order to clarify the mechanism quantitatively, photothermal

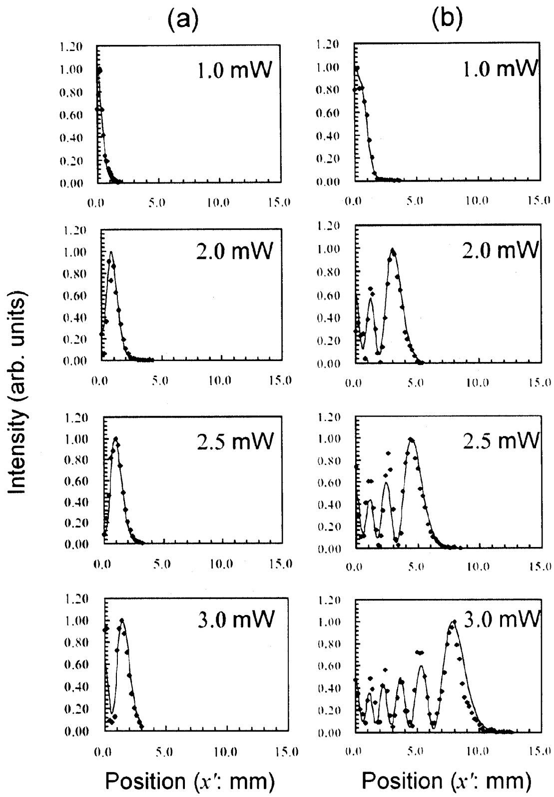

FIGURE 4 Comparison of steady-state radial intensity distributions of the diffracted beam transmitted from the GHLC cells with (a) glass and (b) acrylate substrates. Pump beam intensities were varied and set at 1.0, 2.0, 2.5, and 3.0 mW. Filled circles, experimental data; solid curves, theoretical fitted curves.

self-phase modulation in the GHLC cell was characterized by the three-dimensional heat-conduction analysis. According to Biot-Fourier phenomenological assumption, we obtain the following expression:

$$\rho c \frac{\partial T}{\partial t} = \frac{\partial}{\partial x}\left(k_x \frac{\partial T}{\partial x}\right) + \frac{\partial}{\partial y}\left(k_y \frac{\partial T}{\partial y}\right) + \frac{\partial}{\partial z}\left(k_z \frac{\partial T}{\partial z}\right) + Q(x, y, z) \quad (1)$$

where k_I is known as the thermal conductivity, ρ denotes the density of the media, c is specific heat, and $Q(x, y, z)$ is a heat source which is supplied from the laser beam. In order to solve Equation (1) numerically, we use the finite-element method and obtain both time-dependent and time-independent temperature distribution. In the case of the steady state, we can assume that $\partial T/\partial t$ is zero because the temperature distribution does not depend on time. The detailed method of the three-dimensional heat-conduction analysis was described in our previous study [15,17,18]. Figure 5 shows the calculated temperature distributions with variation of pump beam intensity in the x-axis direction at the boundary between the substrate and the GHLC layer. As the power of the incident laser beam increases, temperature at the beam center ($x = 0$) rises. Notice that the

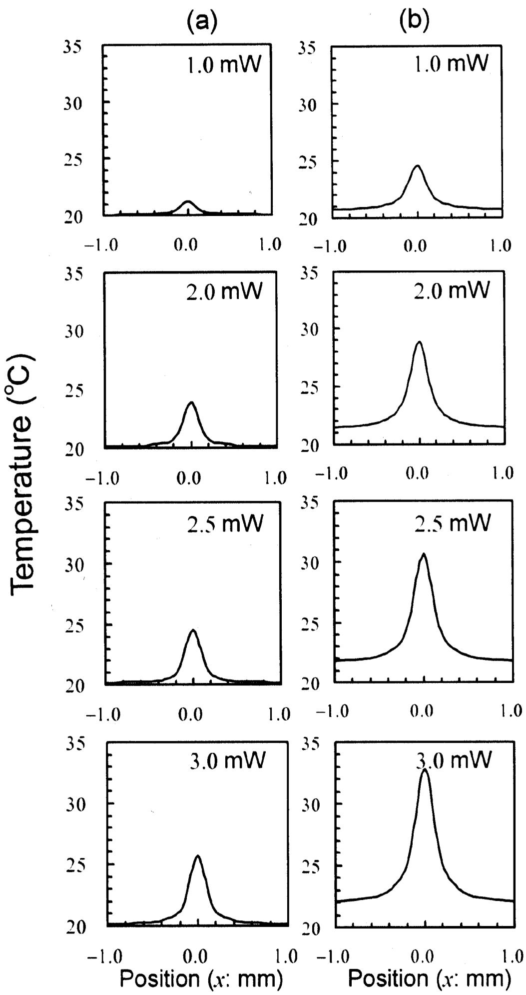

FIGURE 5 Comparison of calculated temperature distributions (x-axis direction) in the GHLC cells with (a) glass and (b) acrylate substrates. Pump beam intensities were varied and set at 1.0, 2.0, 2.5, 3.0 mW.

higher peak temperature was observed in the case of the GHLC cell with the acrylate substrate in comparison with the peak temperature in the case of the GHLC cell with the glass substrate. We attribute that the mechanism of the highly-sensitive photothermal effects of the GHLC cell with the acrylate substrate is linked with the small thermal conductivity of the acrylate substrate. Figure 6 shows the calculated temperature distributions with variation of pump beam intensity in the z-axis direction. In the case of the GHLC cell with the glass substrate (Figure 6(a)), there is the GHLC layer between $z = 1.0$ and $z = 1.1$ mm, while there is the GHLC layer between $z = 2.0$ and $z = 2.1$ mm in the case of the GHLC cell with the

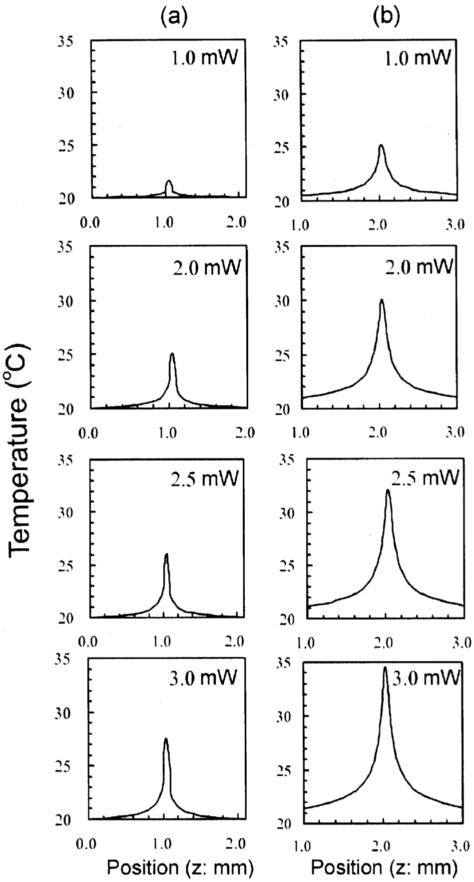

FIGURE 6 Comparison of calculated temperature distributions (z-axis direction) in the GHLC cells with (a) glass and (b) acrylate substrates. Pump beam intensities were varied and set at 1.0, 2.0, 2.5, and 3.0 mW.

acrylate substrate (Figure 6(b)). As shown in the figure, asymmetric distributions were obtained in the z-axis direction since the beam intensity decreases exponentially as the beam propagates in the GHLC layer. In order to estimate the refractive index distribution from the temperature distribution described in Figures 5 and 6, the temperature dependence of the refractive index is needed. For the measurements of temperature dependence of the refractive index we employed standard technique using the wedge cell at the wavelength of 632.8 nm. The detailed method of the index measurements was described in our previous study [15]. We summarize the refractive index change due to the photothermal effects in the GHLC cells with glass and acrylate substrates as a function of the incident light intensity, and the results are shown in Figure 7. The results obtained from the experiments (filled circles and squares) are in good agreement with those from the theoretical calculation (solid and dotted curves). The results support that the physical origin of the photothermal effects in GHLC cells can be well explained by the analytical technique described here. The refractive index change due to the photothermal effects in the GHLCs shows a quadratic dependence in good agreement with the previous results. We attribute the behavior to the large gradient $\partial n_e/\partial T$ which remains in the sample at lower temperature than the nematic-isotropic transition temperature. Since the photothermal effects in the GHLC cell are dependent on the conditions of thermal structure of the GHLC cell, they are highly sensitive to the thermal conductivity of the substrate, as shown in Figure 7. Due to the low thermal conductivity of the acrylate substrate,

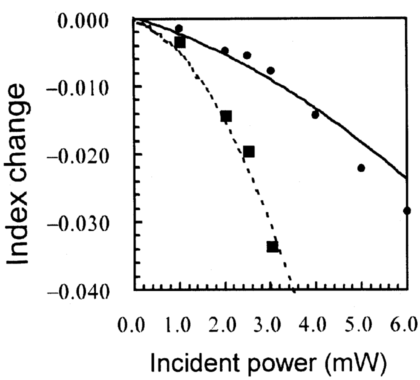

FIGURE 7 Comparison of dependence of the extraordinary refractive-index change in the GHLC cells with glass and acrylate substrates on the pump beam intensity. Filled circles and squares denote experimental data for the GHLC cells with glass and acrylate substrates, respectively. Solid and dotted curves were obtained from the three-dimensional heat-conduction analysis.

the photothermal refractive index change in the GHLC cells with the acrylate substrate could be effectively induced by irradiating a week laser beam to the sample. A more satisfying explanation of these phenomena would require additional information regarding the switching mechanism, and in particular about the transient properties of the thermal conductivity.

The kinetics of photothermal self-phase modulation recording was measured by monitoring temporal evolution of diffraction light intensity after a sudden opening of the input beam. Figure 8 shows the experimental transient fringe signals and theoretical fitted curves obtained from Kirchhoff's diffraction integral, including higher-order optical nonlinearity. One can observe that the power from the center region appeared to be pushed out into the wing region as time passed. Highly sensitive performance of the GHLC cell with the acrylate substrate (Figure 8(b)) is related to the low thermal conductivity of the acrylate substrate, resulting in an increased apparent photothermal activity of the GHLC cell as seen in the transient experiments. In order to clarify the mechanism, Figure 9 shows the contour plots of the temperature distributions, which are obtained from

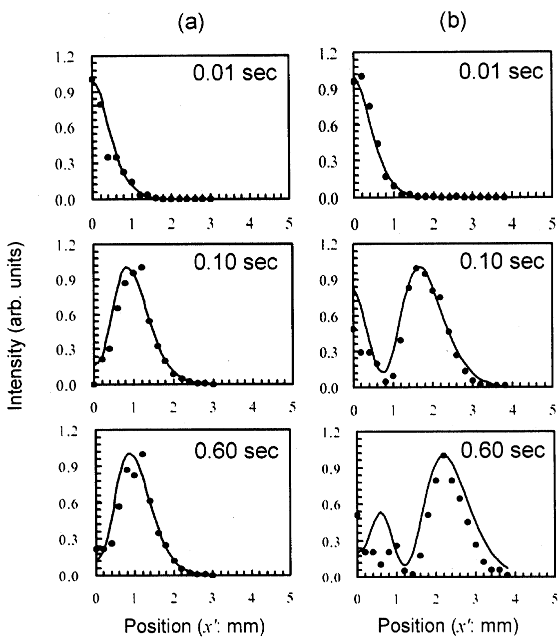

FIGURE 8 Comparison of transient intensity distributions of the diffraction pattern from the GHLC cells with (a) glass and (b) acrylate substrates. Filled circles, experimental data; solid curves, theoretical fitted curves. The beam intensity was 2.0 mW.

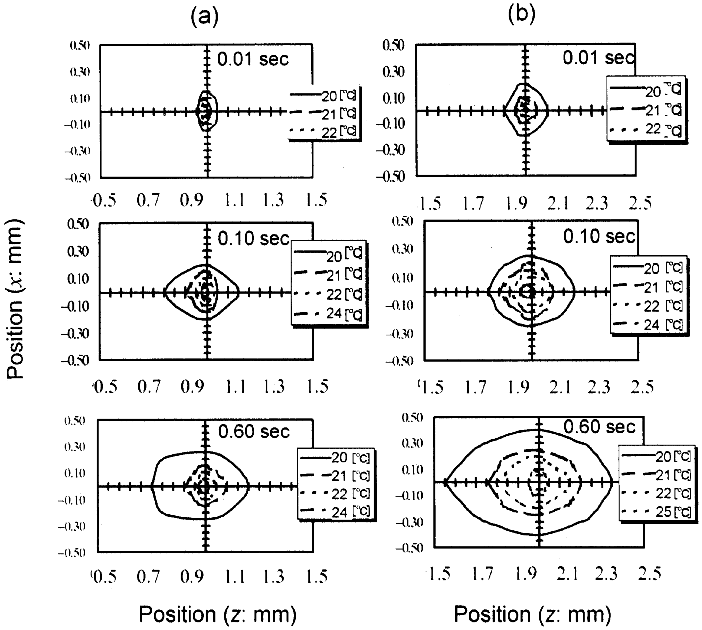

FIGURE 9 Comparison of the contour plots of transient temperature distributions in the GHLC cells with (a) glass and (b) acrylate substrates. The beam intensity was 2.0 mW.

the three-dimensional heat-conduction analysis, with variation of time. One can observe that the heat, which is provided from the laser beam, spread to the wide area as time passed. Since the thermal conductivity of the acrylate substrate is relatively low in comparison with that of the glass substrate as presented in Table 1, the heat is accumulated in the acrylate substrate as shown in Figure 9(b), and the resulting peak temperature in the GHLC cell with the acrylate substrate becomes higher than that in the GHLC cell with the glass substrate. The accumulated heat is used to define a temperature distribution in the GHLC layer, while the temperature change induced is employed for the refractive index change in the GHLC layer. Figure 10 summarizes the time dependence of the peak value of the refractive index change. The agreement between the experimental points and calculated curves are significantly better for the glass substrate than for the acrylate one. One possible explanation for this is that the peak temperature closes to the nematic-isotropic transition temperature in the case of the GHLC cell with acrylate substrate. Since the refractive index drastically changes around the nematic-isotropic transition temperature, the error should be enlarged for the acrylate substrate. First, in order to estimate the rise time

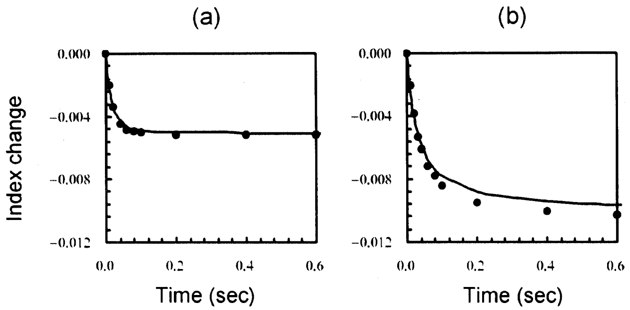

FIGURE 10 Comparison of the transient refractive index change in the GHLC cells with (a) glass and (b) acrylate substrates. Filled circles denote the experimental data and solid curves were obtained from the time-dependent heat-conduction analysis. The beam intensity was 2.0 mW.

of the induced refractive index change, we tried to fit the experimental and theoretical data with the single exponential. However, especially in the case of the transient signals from the GHLC cell with the acrylate substrate, we could not obtain the appropriate solution over the long time range. Next, we tried to fit the data with equation as follows:

$$\Delta n(t) = \Delta n\{1 - a_{fast}\exp(-t/\tau_{fast}) - a_{slow}\exp(-t/\tau_{slow})\}. \qquad (2)$$

Both transient data from the experiments and the time-dependent heat-conduction analysis were well fitted with Equation (2). The physical parameters of the kinetics of the photothermal index change are summarized in Table 2. The transient signals obtained from experiments are in good agreement with those from the time-dependent heat-conduction analysis, despite the fact that the time constants estimated from the theoretical calculation tend to come out slightly faster than those determined directly from the experimental data. The data for the GHLC cell with glass substrate can be fitted with the single exponential function, while the data for the GHLC cell with acrylate substrate cannot be fitted with the single

TABLE 2 Fitting Parameters of Transient Photothermal Index Change

	τ_{fast} [msec]		τ_{slow} [msec]		a_{slow}/a_{fast}	
	Experiment	Theory	Experiment	Theory	Experimet	Theory
Glass	18	14	—	—	0.02	0.01
Acrylate	30	24	201	189	0.67	0.68

Pump beam power was set to be 3.0 mW.

exponential function as described in Table 2. Consequently, in the case of the GHLC cell with the acrylate substrate it is necessary to realize the importance of contributions of the slow heat conduction in the substrate to the total transient properties in the system. The slow component of the transient properties of the photothermal effect is determined by the value of the thermal conductivity of the substrate because the substrate may work as a heat sink which propagates the generated heat to the device surfaces.

CONCLUSIONS

In conclusion, we clarified the relationship between the photothermal effects in the guest-host liquid crystal (GHLC) and the thermal conductivity of the cell substrate. The far-field patterns of a laser beam passed through the GHLC cells were characterized in this study, and we discussed the fact that spatial self-phase modulation induced by a photothermal refractive index change could explain the results. The effects of the thermal conductivity of the cell substrates on the photothermal effects were extensively characterized by two different methods. One method is to analytically solve the Kirchhoff's diffraction integral, including the higher-order nonlinear phase distribution, and to fit the experimental diffraction patterns with theoretical ones. The other approach is to solve the time-independent and time-dependent heat conduction equations and determine the refractive index distributions from the calculated temperature distributions and temperature-dependence of the refractive index of the liquid crystal. The results, including the transient properties from both methods, were in good agreement with each other and the effects of the thermal conductivity of the substrate on the photothermal effects were quantitatively characterized. As described in the introduction to this article, large optical nonlinearity plays a fundamental role in the development of optical and optoelectronic systems for future information technologies. In order to realize the photonics applications using the GHLC, it is very important to investigate the mechanism of laser-induced index change in the GHLC. We hope that the technique described here is useful for separation of photothermal effects and other effects.

REFERENCES

[1] Khoo, I. C. (1995). ***Liquid Crystal***, New York: Wiley.
[2] Durbin, S. D., Arakelian, S. M., & Shen, Y. R. (1981). *Opt. Lett.*, *6*, 411.
[3] Khoo, I. C., & Normandin, R. (1985). *IEEE J. Quant. Electron.*, *QE-21*, 329.
[4] Khoo, I. C., Hou, J. Y., Liu, T. H., Yan, P. Y., Michael, P. R., & Finn, G. M. (1987). *J. Opt. Soc. Am. B*, *4*, 886.

[5] Kurihara, S., Ikeda, T., & Tazuke, S. (1990). *Mol. Cryst. Liq. Cryst.*, *178*, 117.
[6] Darwish, A., Sarkisov, S., Bryant, W., & Ventateswarlu, P. (1995). *SPIE*, *2547*, 258.
[7] Harrison, R. G., Dambly, L., Yu, D., & Lu, W. (1997). *Opt. Commun.*, *139*, 69.
[8] Chen, A. G., & Brady, D. J. (1992). *Opt. Lett.*, *17*, 441.
[9] Inoue, T., & Tomita, Y. (1996). *J. Opt. Soc. Am. B*, *13*, 1916.
[10] Kato, J., Yamaguchi, I., & Tanaka, H. (1996). *Opt. Lett.*, *21*, 767.
[11] Ono, H., & Kawatsuki, N. (1997). *Jpn. J. Appl. Phys.*, *36*, L353.
[12] Ono, H., & Harato, Y. (1999). *J. Appl. Phys.*, *85*, 676.
[13] Macdonald, R., Damerau, U., & Danlewski, H. (1999). *Chaos. Solitons Fractals*, *10*, 651.
[14] Ono, H., & Haroto, Y. (1999). *Appl. Phys. Lett.*, *74*, 3429.
[15] Ono, H., & Haroto, Y. (1999). *J. Opt. Soc. Am. B*, *16*, 2195.
[16] Zhang, H., Shiono, S., Shishido, A., Kanazawa, A., Tsutsumi, O., Shiono, T., & Ikeda, T. (2000). *Adv. Mater.*, *12*, 1336.
[17] Ono, H., & Kikuhara, J. (2000). *Appl. Phys. Lett.*, *76*, 3391.
[18] Ono, H., Harato, Y., & Kikuhara, J. (2000). *Jpn. J. Appl. Phys.*, *39*, 6376.